

# Walking Control Based on Step Timing Adaptation

Majid Khadiv\*, Alexander Herzog<sup>▽</sup>, S. Ali. A. Moosavian<sup>†</sup>, and Ludovic Righetti<sup>\*,○</sup>

**Abstract**—<sup>1</sup> Step adjustment for biped robots has been shown to improve gait robustness, however the adaptation of step timing is often neglected in control strategies because it gives rise to non-convex problems when optimized over several steps. In this paper, we argue that it is not necessary to optimize walking over several steps to guarantee stability and that it is sufficient to merely select the next step timing and location. From this insight, we propose a novel walking pattern generator with linear constraints that optimally selects step location and timing at every control cycle. The resulting controller is computationally simple, yet guarantees that any viable state will remain viable in the future. We propose a swing foot adaptation strategy and show how the approach can be used with an inverse dynamics controller without any explicit control of the center of mass or the foot center of pressure. This is particularly useful for biped robots with limited control authority on their foot center of pressure, such as robots with point feet and robots with passive ankles. Extensive simulations on a humanoid robot with passive ankles subject to external pushes and foot slippage demonstrate the capabilities of the approach in cases where the foot center of pressure cannot be controlled and emphasize the importance of step timing adaptation to stabilize walking.

**Index Terms**—Bipedal locomotion, robust walking, timing adjustment, push recovery, slippage recovery.

## I. INTRODUCTION

DUe to the unilateral nature of feet-ground interaction, legged robots are prone to falling down during their maneuvers. The most important factor in designing walking controllers is therefore to minimize the possibility of falling down even in face of strong perturbations. To achieve stable walking, a controller can act on three different gait aspects: it can decide where to put the feet (step adjustment), when to make a step (step timing adaptation), and how to move the robot's body to manipulate the ground reaction forces (center of pressure (CoP) modulation). Each of these aspects is subject to physical constraints and it is therefore important to optimally modulate each of these variables. State of the art walking pattern generators have mostly focused on the optimal modulation of the CoP (e.g. zero-moment point (ZMP) walking strategies), sometimes in conjunction with foot-step placement or timing adaption. While such strategies afford great flexibility in walking pattern generation, they implicitly assumes high control authority on the end-effectors' CoP.

\*Movement Generation and Control Group, Max-Planck Institute for Intelligent Systems, Germany. e-mail: firstname.lastname@tuebingen.mpg.de

<sup>▽</sup>Google X, email: alexanderherzog001@googlemail.com

<sup>†</sup>Department of Mechanical Engineering, K. N. Toosi University of Technology, Tehran, Iran. e-mail: moosavian@kntu.ac.ir

<sup>○</sup>Department of Electrical and Computer Engineering and Department of Mechanical and Aerospace Engineering, New York University, USA. e-mail: ludovic.righetti@nyu.edu

<sup>1</sup>Part of the material presented in this paper has been presented at the 2016 IEEE/RAS International Conference on Humanoid Robots (Humanoids), [24]

In this paper, we study the problem of optimal step location and timing without explicit control of the feet CoP or the robot center of mass (CoM). This case is relevant for biped robots with no or limited control authority on their CoP: robots with passive ankles, small feet or point feet. It is also of interest for other robots, in order to relax the control constraints on the CoP associated to more traditional preview control algorithms.

### A. Realtime walking pattern generators

Generating walking patterns considering the full robot dynamics allows to reason about multi-contact interactions on complex surfaces [41], [33], [30], [18], [19], [6], [27], [46]. However, this results in high dimensional, non-convex and computationally complex algorithms, therefore limiting their applicability for real-time walking control. To date, most successful approaches for real-time walking control have mostly considered linear models of the CoM dynamics and especially the linear inverted pendulum model (LIPM) [23].

Leveraging analytical solutions of the model, several approaches generate CoM trajectories consistent with a predefined ZMP trajectory [14], [34], [3]. In these approaches, both the position and velocity of the CoM are restricted which constrains both divergent and convergent parts of the LIPM dynamics. In contrast, [40] constrained only the divergent part of the CoM dynamics to generate a trajectory for the divergent component of motion (DCM) based on predefined footprints (ZMP trajectory). Prior to [40], the divergent part of the LIPM dynamics was also used to explain human walking characteristics under the name of extrapolated center of mass (XCoM) [20]. This concept is equivalent to the original Capture Point idea [38], i.e. the point on which the robot should step to come to a stop. In these methods, there is no feedback from the current state of the robot to adapt the CoM motion in the presence of disturbances. To circumvent this, [10] proposed a feedback law to track a DCM trajectory. Although this controller can quickly react to disturbances, perfect DCM tracking assumes unconstrained CoP manipulation.

All of these walking pattern generators can be seen as variants of the same model predictive control (MPC) scheme [45]. One of the pioneering work relating walking pattern generation to optimal control was done by [22]. They proposed a preview control method to generate CoM trajectories based on predefined ZMP trajectories. In this approach, feedback from the current robot state can be used to recompute and adapt the motion online. [43] improved the performance of this approach in the presence of relatively severe pushes, by constraining the motion of the ZMP inside the support polygon rather than predefining a desired ZMP trajectory. The resulting algorithm computes both ZMP and CoM trajectories

respecting feasibility constraints at each control cycle. In all these approaches a preview over several steps is considered for gait planning, but with fixed step locations and timing.

### B. Step adjustment and timing adaptation

Explicit manipulation of the CoP to control the DCM or CoM imposes several restrictions on robot mechanics. Indeed, robots with point contact feet [21] or robots with passive ankles [25] have very limited control authority, if any, on the foot CoP. The modulation of the CoP is also very limited for robots with actuated ankles, due to the rather small foot support area and the limited amount of available ankle torque. This is in contrast to step adjustment, which allows to select the next step location in a relatively large area compared to the support polygon. It constitutes therefore a more significant tool for stabilizing biped walking. Step adaptation algorithms [9], [10], [25], [8], [15], [16], [12] make walking pattern generators more robust against disturbances. However, in these methods step timing is never adapted. Indeed, it is necessary to fix step duration to keep the problem convex over a sequence of several footsteps.

In [11], it was shown that using a combination of step location and timing adaptation increases significantly the basin of attraction for bipedal locomotion. [32] proposed an analytical method for computing nominal gait variables for a desired walking velocity, and an algorithm for adapting both step location and timing based on heuristics. [7] proposed an analytical method for step timing and foot placement adaptation based on the CoM state feedback, with a priority given to the sagittal gait. [13] modified the analytical approach in [10] by adjusting both step location and timing. They used step location and timing adjustment using heuristics to compensate for the DCM (or instantaneous capture point (ICP)) tracking error. Apart from adjusting step timing to robustify gaits against disturbances, [35], [26] adapted the single support duration to negotiate soon or late landing of the swing foot using contact detection.

Step duration was also used as an optimization variables in [1], [29]. However, these approaches result in non-convex optimization problems which are computationally expensive and do not guarantee convergence to a global minimum. [31] proposed an extension of the gait planning approach in [15] to adjust step duration. They related the problem through a mixed-integer quadratic program (MIQP) which has combinatorial complexity. Furthermore, [5], [4] used timing adaptation to limit the acceleration of the swing foot, during walking on uneven terrains.

### C. Viability and capturability constraints

Viability theory [2] is an appealing framework to discuss the stability of walking. The viability kernel includes all the states from which it is possible to avoid falling [42]. Computing this kernel is generally not tractable but it has been argued in [44] that it is sufficient to limit an integral of the states of the system over several previewed steps to guarantee walking long-term stability [45]. In general, viability can be guaranteed by setting a terminal condition on the states in a previewed number of

steps as a sufficient condition [40], [10], or by minimizing other forms of viability [22], [43], [15]. As a result, the majority of walking pattern generators today consider several steps of preview to optimize walking as we discussed above.

Capturability, i.e. the ability to come to a stop after a certain number of steps, is a concept developed in [38]. In [28], an extensive capturability analysis is performed for the LIPM and its extension. In particular, a bound for the infinite-step capturability set is computed, which is equivalent to computing the viability set of the LIPM. It is a very valuable result, as this can guarantee viability without the need to consider several walking steps, therefore significantly simplifying the walking pattern generator problem. To the best of our knowledge, this bound has never been used to synthesize a walking pattern generator.

### D. Contributions of the paper

In this paper, we use results characterizing the viability kernel of the LIPM [28] to argue that it is sufficient to solely decide for the next step location and timing to ensure walking stability from any viable state. This means that adding a longer preview of steps does not improve the capability of the LIPM to reject disturbances as long as both step timing and location are adapted for the next step. To the best of our knowledge, this insight has not been exploited in control synthesis, as state of the art preview control approaches include stability constraints over a preview of several steps despite it being unnecessary and computationally more complex.

We use this insight to design a model predictive controller optimizing the next step location and, most importantly, timing at every control cycle while guaranteeing walking stability from any currently viable state. We then investigate the importance of step timing adaptation for walking stability. The algorithm is formulated as a quadratic program with a very low number of decision variables. It contains at least an order of magnitude less decision variables than state of the art algorithms such as [16]. To the best of our knowledge, it is the first algorithm able to adapt step timing and location at the same time while keeping the problem convex. Moreover, the algorithm does not rely on CoP modulation, which makes it applicable to any biped robots, including robots with passive ankles and point feet.

We then propose a simple strategy to adapt online Cartesian swing foot trajectories to follow the adapted step timing and location. Extensive simulations on a full humanoid robot with passive ankles using hierarchical inverse dynamics [17] demonstrate the capabilities of the approach for robots with limited control authority on the CoP. In particular, our experiments emphasize the importance of timing adaptation during walking. Interestingly, the full body controller does not require an explicit control of the CoP nor of the CoM horizontal motion. As a result, our approach allows the robot to handle a significant amount of disturbances including external pushes and foot slippage.

This paper extends our preliminary work [24] with a discussion on the properties of our algorithm with respect to viability. We study the influence of timing adaptation for disturbance

recovery. In particular, we present more extensive simulation experiments of a full humanoid robot with passive ankles including push and foot slippage experiments.

### E. Organization of the paper

Section II recalls fundamental results about the DCM and viability. Section III introduces the walking controller for optimal adjustment of step location and timing. Section IV describes the integration of the walking controller in the whole-body controller. Section V shows extensive results for the LIP model and compares our controller with state of the art preview controllers. Section VI is dedicated to full humanoid simulations on various scenarios. We discuss the results and conclude in Section VII and VIII.

## II. PROBLEM FORMULATION AND VIABILITY

In this section, we recall previous results on the LIPM, the DCM and the viability of the model. We also present a convenient change of variable, the DCM offset, to express the viability constraint in a form convenient to synthesize our stepping controller.

The LIPM constrains motion of the CoM on a plane (horizontal plane for walking on a flat surface), by using a telescopic massless link connecting the CoP to the CoM [23]. The dynamics of this system may be formulated as

$$\ddot{x} = \omega_0^2(x - u_0) \quad (1)$$

where  $x \in \mathbb{R}^2$  is the CoM horizontal position (the vertical component has a fixed value  $z_0$ ), and  $u_0 = [CoP_x, CoP_y]^T$  is the CoP position on the floor. For point contact feet,  $u_0$  is identical to the contact point.  $\omega_0$  is the natural frequency of the pendulum ( $\omega_0 = \sqrt{g/z_0}$ , where  $g$  is the gravity constant and  $z_0$  the CoM height). Defining the DCM as  $\xi = x + \dot{x}/\omega_0$ , the LIPM dynamics can also be written as [9]

$$\dot{x} = \omega_0(\xi - x) \quad (2a)$$

$$\dot{\xi} = \omega_0(\xi - u_0) \quad (2b)$$

Equation (2) explicitly reveals the stable and unstable parts of the LIPM dynamics, where the CoM converges to the DCM (Eq. (2a)) and the DCM is pushed away by the CoP (Eq. (2b)).

By solving (2b) as an initial value problem, the DCM motion based on the natural dynamics of the LIPM is written

$$\xi(t) = (\xi_0 - u_0)e^{\omega_0 t} + u_0 \quad (3)$$

The DCM at the end of a step of duration  $T$  is

$$\xi_T = (\xi_0 - u_0)e^{\omega_0 T} + u_0 \quad (4)$$

This representation is very convenient, as is sufficient to constraint the DCM motion without considering the stable part to ensure stable walking, for example by constraining the DCM location at the end of a specified time  $\xi(T)$  as in [10]. In this case, a terminal condition (captured state) is set at the end of a predefined number of steps, and the desired DCM at the end of the current step is recursively computed.

This is not the only way to keep the DCM from diverging. In fact, a legged robot can instantaneously change its CoP

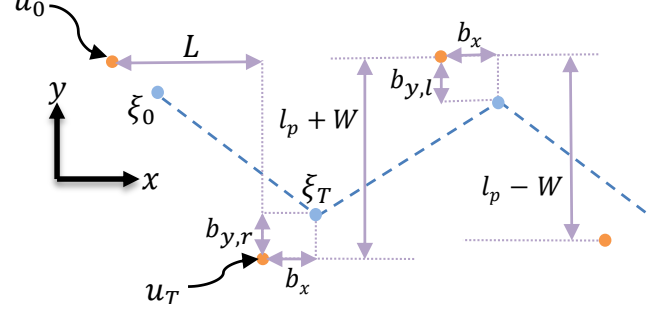


Fig. 1. A schematic view of the walking pattern showing the footprints, the DCM, and the DCM offset

location  $u_0$  by taking a step [28] in order to limit the DCM motion. This is for example the approach taken in [38]. In [28], it was shown that the  $\infty$ -step capturability region was solely a function of the maximum step length and minimum step time. Therefore, any viable state will remain viable as long as the next step timing and location satisfy this  $\infty$ -step capturability constraint. It is the approach we exploit in this paper.

### A. The DCM offset

We first introduce the DCM offset which is a convenient change of variable to synthesize controllers that enforce a desired CoM average velocity. We also compute the maximum DCM offset bound that preserves viability. It is defined as

$$b = \xi_T - u_T \quad (5)$$

where  $u_T$  is the next step location and  $\xi_T$  the DCM at the end of the step (Figure 1). The LIPM solution can be written in terms of the next footprint location, the step duration and the DCM offset by solving Equation (2b) as a final value problem

$$u_T = (\xi_{cur} - u_0)e^{\omega_0(T-t)} + u_0 - b \quad , \quad 0 \leq t \leq T \quad (6)$$

in which  $\xi_{cur}$  is the current DCM of the robot. Bounding the DCM offset at the end of a step will guarantee the viability of walking. Furthermore, the DCM offset is convenient as it allows to also enforce a desired forward velocity. Assume that a desired CoM average velocity is given by a desired step length  $L$ , width  $W$  and a desired step duration  $T$ . The desired DCM offset in the sagittal and lateral directions that achieve the desired velocity is <sup>2</sup>

$$b_x = \frac{L}{e^{\omega_0 T} - 1} \quad (7a)$$

$$b_y = (-1)^n \frac{l_p}{1 + e^{\omega_0 T}} - \frac{W}{1 - e^{\omega_0 T}} \quad (7b)$$

where  $l_p$  is the default step width and  $n$  is an index that distinguishes left and right feet ( $n = 1$  when the right foot is stance, and  $n = 2$  when the left foot is stance). Note that  $W$  is the deviation of the step width with respect to the pelvis width. In fact, this value shows how much the robot moves laterally, so we will call it the *step width* (Figure 1).

<sup>2</sup>cf. Appendix A for the derivation details

### B. Viability bound on the DCM offset

We now want to express the viability region for the LIPM model [2], [42], [44] in terms of the DCM offset. Viability is generally intractable but fortunately, it is possible to characterize these bounds for the LIPM as it was first shown in [28] where the viability was characterized in terms of the  $\infty$ -step capturability region (i.e. the region of the DCM where the system remains capturable by an infinite number of steps). It is written as

$$d_{\infty} = L_{\max} \frac{e^{-\omega_0 T_{\min}}}{1 - e^{-\omega_0 T_{\min}}} \quad (8)$$

where  $L_{\max}$  and  $T_{\min}$  are the maximum step length and minimum step duration, respectively.

Equation (8) allows to analyze the viability of the current state of the system but is not necessarily convenient to relate viability to the next step location and duration. Moreover, the best of our knowledge, this bound has not been used to ensure walking stability. Indeed, walking pattern generators typically enforce walking stability by imposing a terminal constraint after several preview steps [45].

Now, we write the viability bounds in terms of the DCM offset. We limit our analysis to the sagittal plane dynamics for forward walking (analysis of backward walking is similar and the lateral direction analysis is given in Appendix B). The maximum DCM offset is related to the maximum step length and minimum step duration as

$$b_{x,\max} = \frac{L_{\max}}{e^{\omega_0 T_{\min}} - 1} \quad (9)$$

We show now that this maximum offset also characterize viable and non-viable states. We consider two cases: I) if the DCM offset is larger than  $b_{x,\max}$ , we show that all possible choices of step timing and location lead to its divergence and II) we show that for DCM offsets smaller than  $b_{x,\max}$ , there exists at least one combination of step timing and location that keeps the DCM from diverging.

*Case I:* If the DCM offset is larger than  $b_{x,\max}$  at the start of a step then

$$\xi_{x,0} - u_{x,0} = \frac{L_{\max}}{e^{\omega_0 T_{\min}} - 1} + \epsilon \quad (10)$$

where  $\epsilon$  is an arbitrary positive number. Using Equations (4), (5) and (10), the DCM offset at the end of the step is

$$b_x = \left( \frac{L_{\max}}{e^{\omega_0 T_{\min}} - 1} + \epsilon \right) e^{\omega_0 T} - (u_{x,T} - u_{x,0}) \quad (11)$$

Substituting  $u_{x,T} - u_{x,0} = L_{\max}$  and  $T = T_{\min}$ , the minimum realizable offset  $b_x$  is therefore

$$b_x = \frac{L_{\max}}{e^{\omega_0 T_{\min}} - 1} + \epsilon e^{\omega_0 T_{\min}} \quad (12)$$

Comparing Equations (10) and (12), we see that the minimum realizable DCM offset at the end of the step increases by  $e^{\omega_0 T_{\min}}$ . A sequence of steps will therefore result in a divergent geometric series with common ratio  $e^{\omega_0 T_{\min}}$ . Therefore, all possible choices of step location and timing starting from a DCM offset larger than  $b_{x,\max}$  lead to divergence (i.e. a fall).

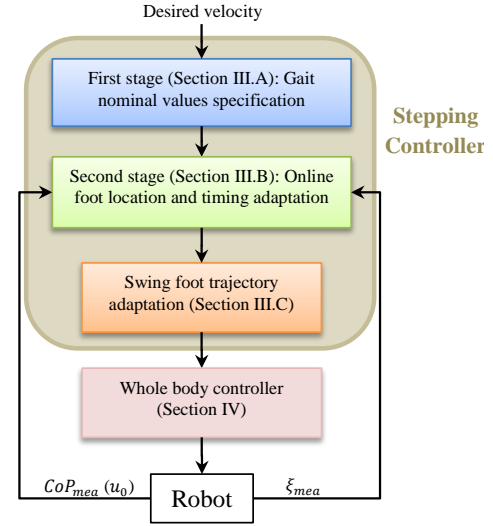


Fig. 2. Block diagram of the walking algorithm. Refer to Section III for a detailed description of each component.

*Case II:* If the DCM offset is smaller than  $b_{x,\max}$  at the start of a step then

$$\xi_{x,0} - u_{x,0} \leq \frac{L_{\max}}{e^{\omega_0 T_{\min}} - 1} \quad (13)$$

Using Equations (4), (5) and (13), we obtain the following constraint on the DCM offset

$$b_x \leq \left( \frac{L_{\max}}{e^{\omega_0 T_{\min}} - 1} \right) e^{\omega_0 T} - (u_{x,T} - u_{x,0}) \quad (14)$$

Selecting the next step position and timing as  $u_{x,T} - u_{x,0} = L_{\max}$  and  $T = T_{\min}$ , we find

$$b_x \leq \frac{L_{\max}}{e^{\omega_0 T_{\min}} - 1} \quad (15)$$

Comparing Equations (13) and (15), we see that starting from a state satisfying Equation (13), there exists at least one choice of step position and timing that keeps the DCM offset bounded at the end of the next step: this state is viable.

**Remark** The DCM offset bound is equivalent to the  $\infty$ -step capturability bound derived in [28]. However, the DCM offset bound is particularly convenient to optimize the next step location and timing in a walking controller that 1) enforce a desired CoM velocity and 2) guarantees viability, which we present in the next section.

### III. STEPPING CONTROLLER

The stepping controller is comprised of three stages depicted in Figure 2. First, we compute nominal values for the step location, step duration, and the DCM offset for a desired walking velocity. Second, these nominal values are used to compute optimal desired step duration and location at each control cycle. Finally, step duration and location are exploited to constantly adapt swing foot trajectories that are then used by a whole body controller to generate walking (Section IV).

### A. First stage: nominal values for stepping

In the first stage, we use the procedure described in [24] to find gait variables consistent with a desired walking velocity. In fact, in this stage we aim to find a desired set of step length and width as well as step duration that satisfies the robot and environment constraints. Hence, the problem is to find the nominal step length  $L_{nom}$ , step width  $W_{nom}$ , and step duration  $T_{nom}$ , subject to kinematic and dynamic constraints

$$\begin{aligned} v_x &= \frac{L_{nom}}{T_{nom}}, & v_y &= \frac{W_{nom}}{T_{nom}} \\ L_{min} &\leq L_{nom} \leq L_{max} \\ W_{min} &\leq W_{nom} \leq W_{max} \\ T_{min} &\leq T_{nom} \leq T_{max} \end{aligned} \quad (16)$$

where  $v_x$  and  $v_y$  are the desired average walking velocities in sagittal and lateral directions. The step location bounds,  $L_{min}$ ,  $L_{max}$ ,  $W_{min}$  and  $W_{max}$ , are decided by the user and result from a combination of the robot (limited step length and width) and environment (limited area for stepping) limitations. The minimum step timing limits the acceleration of the swing foot and the maximum step timing limits slow stepping.

There are several possible combinations of step length and time that achieve a desired CoM velocity. Here we compute the gait nominal values such that they are as far as possible from boundaries

$$\begin{aligned} T_{nom} &= \frac{B_l + B_u}{2} \\ L_{nom} &= v_x \left( \frac{B_l + B_u}{2} \right) \\ W_{nom} &= v_y \left( \frac{B_l + B_u}{2} \right) \end{aligned} \quad (17)$$

where we chose (cf. [24] for more details)

$$\begin{aligned} B_l &= \max \left\{ \frac{L_{min}}{|v_x|}, \frac{W_{min}}{|v_y|}, T_{min} \right\}, \quad v_x, v_y \neq 0 \\ B_u &= \min \left\{ \frac{L_{max}}{|v_x|}, \frac{W_{max}}{|v_y|}, T_{max} \right\}, \quad v_x, v_y \neq 0 \end{aligned}$$

Notice that we use  $B_l = T_{min}$  and  $B_u = T_{max}$ , when  $v_x, v_y = 0$ . We can then compute the desired DCM offsets corresponding to these nominal values using Equation (7).

### B. Second stage: online foot location and timing adaptation

The second stage of the algorithm adapts the gait characteristics based on the DCM measurement at each control cycle (typically 1KHz on a torque controlled robot) by using the step length, width and duration nominal values to achieve a desired CoM velocity. The algorithm computes step location and timing as close as possible to the nominal values while enforcing viability constraints.

The LIPM solution can be written in terms of the next footprint location, the step duration, and the DCM offset using Equation (6). In order to have a linear relation between timing and step location, we use the following exponential transformation for the step timing

$$\tau = e^{\omega_0 T} \implies T = \frac{1}{\omega_0} \log(\tau) \quad (18)$$

Equation (6) is now linear in the decision variables  $\tau$ ,  $b$ ,  $u_T$

$$u_T - (\xi_{mea} - u_0) e^{-\omega_0 t} \tau + b = u_0 \quad , \quad 0 \leq t \leq T \quad (19)$$

here  $t$  is the time elapsed since the beginning of the swing phase. The actual step duration is recovered through the logarithmic transformation in Equation (18). We can now write the step adaptation problem as a quadratic program

$$\begin{aligned} \min_{u_T, \tau, b, \psi} \quad & \alpha_1 \|u_T - \begin{bmatrix} L_{nom} \\ W_{nom} \end{bmatrix}\|^2 + \alpha_2 |\tau - \tau_{nom}|^2 \\ & + \alpha_3 \|b - \begin{bmatrix} b_{x,nom} \\ b_{y,nom} \end{bmatrix}\|^2 + \alpha_4 \|\psi\|^2 \\ \text{s.t.} \quad & \begin{bmatrix} L_{min} \\ W_{min} \end{bmatrix} \leq u_T \leq \begin{bmatrix} L_{max} \\ W_{max} \end{bmatrix} \\ & e^{\omega_0 T_{min}} \leq \tau \leq e^{\omega_0 T_{max}} \\ & u_T + b = (\xi_{mea} - u_0) e^{-\omega_0 t} \tau + u_0 \\ & \begin{bmatrix} b_{x,min} + \psi_1 \\ b_{y,max,out} + \psi_3 \end{bmatrix} \leq b \leq \begin{bmatrix} b_{x,max} + \psi_2 \\ b_{y,max,in} + \psi_4 \end{bmatrix} \end{aligned} \quad (20)$$

where the last inequality is the viability condition, which is treated as a soft constraint using the slack vector  $\psi = [\psi_1 \psi_2 \psi_3 \psi_4]^T$  (cf. Appendix B for  $b_{y,max,in}$  and  $b_{y,max,out}$  definitions).

In practice, we choose a very high  $\alpha_4$  to give the highest priority to the constraint while guaranteeing that the program will always return a solution even if viability cannot be maintained<sup>3</sup>. This program finds step duration, location and DCM offset as close as possible to the nominal values while enforcing viability as a soft constraint. In the following we also use a large weight for the nominal DCM offset cost with respect to step location and time costs to favor solutions close to the desired walking speed. With these weight choices, the optimizer automatically favor solutions that converge after fewer steps to the nominal walking speed without the need to specify any number of steps. When the nominal DCM offset cannot be achieved, more than one step will be required to converge back to the nominal walking speed. Also, thanks to the viability constraint, it will recover from any disturbances as long as the robot is in a viable state. We note that for the LIPM it is therefore not possible to find a stepping-based controller that performs better in terms of disturbance recovery.

### C. Third stage: Swing foot trajectory adaptation

As the step locating and timing varies at each control cycle, it is necessary to adapt the swing foot trajectory accordingly at the same frequency. We propose here a method to adapt the swing foot trajectory that is computationally simple while guaranteeing smooth swing foot motion.

In the directions horizontal to the ground, we consider fifth order polynomials such that the trajectories are continuous at the order of acceleration to ensure smooth control policies when used in an inverse dynamics control law [17]. In the vertical direction, the problem is a bit more complicated. Indeed, the swing foot height increases until the middle of the step and then decreases smoothly to land on the ground.

<sup>3</sup>The viability constraint could be strictly enforced with a lexicographic optimization approach but it makes little difference in practice with high  $\alpha_4$ .

In this case, one could use two fifth order polynomials for the two parts of the trajectory: one to connect the the prior state to the desired mid-swing foot height and the other to move the leg on the ground at the end of the swing phase. However, such a straightforward approach has two important problems. First, a change of step timing in the vicinity of the mid-time can cause a jump from the first spline to the second one. Second, a change of step timing in the second part generates unavoidable fluctuations in the vertical direction which may cause collision of the swing foot with the ground.

In this paper, we consider instead a 9th order polynomial for the whole step. The problem is to find the polynomials coefficients such that the swing foot height at the mid-time of the step is as close as possible to the desired height. Furthermore, the swing foot height during the step should be strictly positive and lower than a maximum height. The polynomial coefficients are found by solving the following quadratic program

$$\begin{aligned} \min_{c_i} \quad & \|z(T/2) - z_{des}\|^2 \\ \text{s.t.} \quad & 0 \leq z(t) \leq z_{max} \\ & z(0) = 0 \quad z(t_{k-1}) = z_{k-1} \quad z(T) = 0 \quad (21) \\ & \dot{z}(0) = 0 \quad \dot{z}(t_{k-1}) = \dot{z}_{k-1} \quad \dot{z}(T) = 0 \\ & \ddot{z}(0) = 0 \quad \ddot{z}(t_{k-1}) = \ddot{z}_{k-1} \quad \ddot{z}(T) = 0 \end{aligned}$$

In this equation  $z$  is the vertical component of the swing foot. By solving this equation, the polynomial coefficients  $c_i$ 's are obtained at each control cycle. Then, by evaluating the polynomial at the current time, the desired foot trajectory is obtained in real-time.

#### IV. WHOLE BODY CONTROL

We use a hierarchical inverse dynamics controller described in [17] to control the desired swing foot motions computed in the previous section. This controller allows to specify a hierarchy of desired task space behaviors and constraints expressed as linear equalities and inequalities where it computes the optimal joint accelerations, contact forces and actuation torques to achieve them. The equations of motion and actuation limits (i.e. physical consistency) are in the highest priority. The equations of motion can be written as

$$M(q)\ddot{q} + N(q, \dot{q}) = S^T \tau + J_c^T \lambda \quad (22)$$

where  $M$  is the robot inertia matrix,  $q \in \mathbb{R}^n \times SE(3)$  is the vector of generalized coordinates, and  $N$  groups together the Coriolis, centrifugal and gravitational effects.  $S$  represents the joint selection matrix,  $\tau$  is the vector of actuation torques,  $J_c$  is the contact Jacobian, and  $\lambda$  is the vector of generalized contact forces. In the following, we describe the tasks and constraints used with the controller, the details of the controller can be found in [17].

##### A. Foot trajectory tracking

The swing foot tracking task ensures that the desired motions computed in Section III-C are properly executed on the robot. This task is written as

$$J_{sw}\ddot{q} + \dot{J}_{sw}\dot{q} = \ddot{X}_d + K_d(\dot{X}_d - \dot{X}) + K_p(X_d - X) \quad (23)$$

where  $X$  and  $X_d$  are the actual and reference swing foot positions, and  $J_{sw}$  is the swing foot Jacobian.  $K_p$  and  $K_d$  are diagonal gain matrices. It should be noted that we do not control the orientation of the swing foot because we will use a simulation of a robot with passive ankles and there is not enough DOFs to control the orientation. For the stance foot, the task is to remain on the ground

$$J_{st}\ddot{q} + \dot{J}_{st}\dot{q} = 0 \quad (24)$$

where  $J_{st}$  is the stance foot Jacobian. This task keeps the stance foot in a stationary contact with the ground surface.

##### B. Center of Mass height tracking

While it is not necessary to control the horizontal motion of the center of mass, we need a task to keep a desired center of mass height. We use the following task

$$J_{CoM}\ddot{q} + \dot{J}_{CoM}\dot{q} = K_p(z_d - z) - K_d\dot{z} \quad (25)$$

where  $J_{CoM}$  is the CoM height Jacobian,  $z$  is the CoM height and  $z_d$  is set to the CoM height used in the LIPM ( $z_d = z_0$ ).

##### C. Posture control

For proper redundancy resolution and to ensure that the robot keeps a straight posture, we use the following posture task

$$\ddot{q} = K_p(q_d - q) - K_d\dot{q} \quad (26)$$

where  $K_p$  and  $K_d$  are diagonal gain matrices of the actuated joint dimensions.

##### D. Force regularization

In the case of redundancy in actuation (e.g. during the double support phase), we ask the optimizer to compute contact forces as close as possible to desired forces that distribute the weight of the robot among the contacts while staying away from the friction cones limits. This task is not relevant during swing phases.

##### E. Task hierarchy

The hierarchical inverse dynamics controller offers to possibility to specify a hierarchy between tasks, ensuring that tasks of higher priority are not disturbed by lower priority tasks. The hierarchy used for all the experiments presented in this paper is specified in Table I. We give the highest priority to physical consistency and actuation limits. The second rank enforces contact constraints for the stance foot and CoM height. Again, we emphasize that the horizontal motion of the CoM is not controlled. The swing foot control, which essentially generates the walking motions is in the third rank. The last two ranks are used for the posture control and force regularization (which is only relevant during double support phases).

#### V. LIPM MODEL SIMULATION

In this section, we present simulation results using a simulation of the LIPM model. First, we study the push recovery capabilities of our controller and show that step timing adaptation indeed significantly increases these capabilities. Second, we compare our controller with a state of the art of preview control [15] in terms of robustness against pushes.

TABLE I  
HIERARCHY OF TASKS USED IN THE HUMANOID SIMULATION.

Rank	Nr. of eq/ineq constraints	Constraint/Task
1	6 eq	Newton Euler equations
	$2 \times 4$ ineq	Torque limits
2	6 eq	Stance foot constraint
	1 eq	CoM height control
3	3 eq	Swing foot control
4	$2 \times 4$ eq	Posture Control
5	$2 \times 6$ eq	Force regularization

### A. Simulation results using the LIPM

In the first scenario, we consider the LIPM abstraction of a robot walking with a set desired velocity. Footsteps and swing foot trajectories are computed as described in Section III. During each step, the stance foot is considered as the point of contact of the LIPM. At the end of a step where the point of contact of the LIPM is changed, the foot index  $n$  is changed. By changing the foot index, the feasible area is computed for the new step location. We apply pushes on the robot and compare the recovery capabilities of our proposed controller to the case where no step timing adjustment is employed. The robot mass is 60 Kg and the CoM height is 80 cm, Table II (the step location limitations are specified with respect to the stance foot). These properties correspond to a real Sarcos humanoid robot (Figure 5).

TABLE II  
PHYSICAL PROPERTIES OF THE ABSTRACT MODEL.

Value	Description	min	max
$L$	Step length	-50 cm	50 cm
$W_{right}$	Step width (right)	-10 cm	20 cm
$W_{left}$	Step width (left)	-20 cm	10 cm
$T$	Step duration	0.2 sec	0.8 sec

We compare our controller with one using fixed step duration  $T_{nom}$ . In this scenario, we set a forward desired velocity ( $v_x = 1m/s$ ). Based on the limitations specified in Table II, the first stage of our proposed method generates the nominal step length and step duration (Equation (17)), as well as the nominal DCM offset (Equation (7)). After four steps, the robot is pushed at  $t = 1.4s$  to the right direction with a force  $F = 325N$ , during  $\Delta t = 0.1s$ . We conduct two simulations to compare the results of fixed and optimized step duration. In case (a), we use Equation (6) for the step adjustment, using the current DCM measurement. In case (b), we solve the optimization problem in Equation (20) at each control cycle to generate the desired time and location of the next step.

Figure 3 illustrates the resulting trajectories for each case. As it can be observed in the top figures, for the case without timing adjustment (case (a)), the robot steps on the borders of feasible area to recover from the push. But, since in this case stepping can be realized only at fixed times, as time goes the DCM diverges and the swing foot is not able to capture the DCM fast enough. However, when timing adjustment is enabled (case(b)), the algorithm adapts the next footprint and landing time based on the measured DCM. As a result, the robot steps on the borders of the feasible area very fast to recover from the push. In the bottom figures, the swing foot

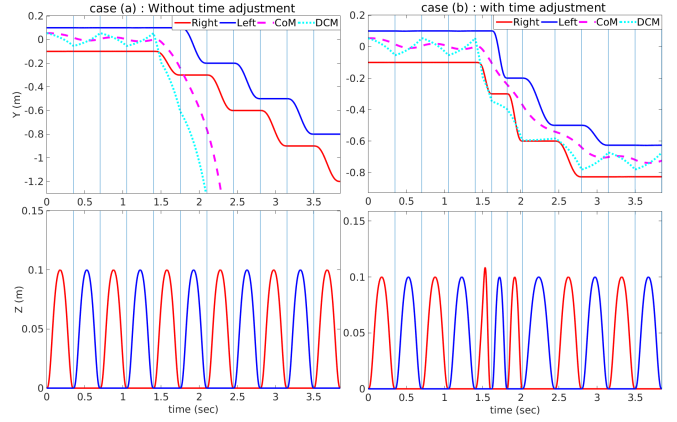


Fig. 3. Comparison of trajectories in cases with and without time adjustment. Top: left and right feet, CoM and DCM horizontal positions. Bottom: left and right feet height. The vertical lines show the step duration.

trajectory in vertical direction for each case is shown. As it can be observed, employing the constrained problem in Equation (21) results in very smooth swing foot trajectories, despite the constant step location and timing adjustment.

### B. Comparison with a state of the art preview controller

In the second scenario, we compare the robustness of our proposed optimization procedure with time adjustment to the approach proposed in [15]. We choose this algorithm for comparison because it can be considered, together with variations of this technique [22], [43], [8] as a standard, state of the art, walking pattern generator. The optimizer in [15] is an extension of the algorithms developed in [22], [43], [8] which generates automatically both step locations and CoM trajectory for a desired walking velocity. Since in this approach the next step locations are considered as decision variables, the optimizer adapts step locations inside a feasible area while step timing is fixed. In the paper, a horizon of  $N = 16$  time intervals of length  $T = 0.1s$  is used, which results in a total preview horizon of  $NT = 1.6s$ . Note also that solving the quadratic program for this problem with a 1.6 s horizon is considerably more expensive compared to our approach in terms of computation cost.

We used the same parameters for both approaches using a LIPM with point contact and computed the maximum push that each approach can recover from in various directions (Figure 4). The value  $\theta$  is the angle between the direction of motion and the push direction (counterclockwise). Hence, negative values show pushes to the right direction. We present here stepping with zero forward velocity to have symmetric results, but qualitatively similar results are obtained at different walking velocities. For each simulation, a force during  $\Delta t = 0.1s$  is applied at the start of a step in which the left foot is stance. We use  $T_{nom} = 0.5s$  (computed from the first stage of our algorithm) for both approaches.

As it can be observed in Figure 4, our walking controller which solves a small sized quadratic program and only adapts the next step location and time can recover from much more severe pushes compared to the approach in [15] with a preview of several steps but without step timing adaptation. It can

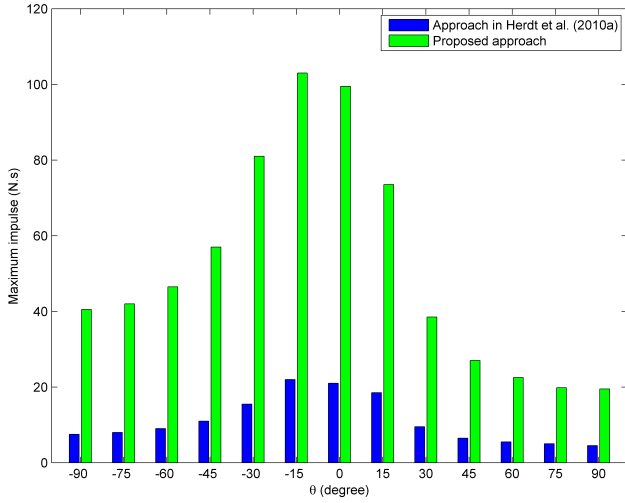


Fig. 4. Comparison with the controller from [15].  $\theta$  is the angle between the direction of motion and the push direction (counterclockwise).  $\theta = 0$  deg corresponds to a forward push, while  $\theta = 90$  deg and  $\theta = -90$  deg represent pushes to the left and right directions, respectively. Backward pushes are not shown as they result in symmetric results.

be seen that for the side pushes, the direction of the push affects the maximum value of the push that the robot is able to recover from. Indeed, for certain pushes the robot is prone to experience a self-collision (we name it outward direction, left in this case with positive  $\theta$  values) and the feasible stepping area is more limited than the other direction (inward direction). We notice that the maximum push in the direction  $\theta = -15$  deg (outer corner of the rectangle of feasible area) is larger than the other directions because the feasible area for stepping in this direction is larger than the other directions.

We also tested the controller of [15] when utilizing the minimum step timing  $T_{min}$ . Here we obtain the exact same robustness results as in our approach. In fact, in the case of a very severe push, both algorithms yield stepping on the boundaries of the feasible area at the minimum step timing. The difference is that in our approach stepping is done at the nominal timing as far as possible from boundaries. It is only in the case of a disturbance that step timing is adapted. Stepping always with minimum time can be an issue as the possibility of system failure increases. Indeed, in this case actuators will work at their maximum capability all the time and augment the risk of failure. Furthermore, the number of switching between the feet increases which makes the system more vulnerable to lose its balance due to surface unevenness. The other problem caused by stepping with the minimum step timing as a nominal behavior is a great decrease in energy efficiency. In contrast, our algorithm will create steps at maximum speed only in case of absolute necessity which is a more desirable behavior.

## VI. HUMANOID WITH PASSIVE ANKLES SIMULATION

In this section, we use our walking controller on a physical simulation of a Sarcos humanoid robot (Figure 5). Each leg of the robot has 4 active degrees of freedom with passive ankle joints and prosthetic feet. For simulating the passive ankle joints, stiff springs and dampers are used. The actuation

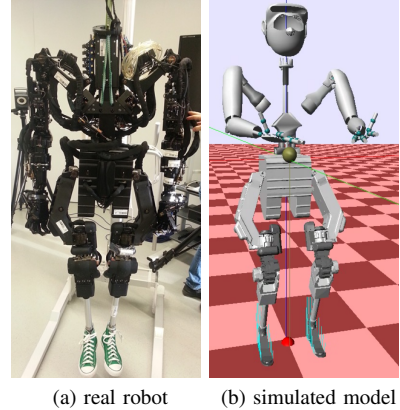


Fig. 5. Sarcos humanoid robot with passive ankles and prosthetic feet used in our simulations.

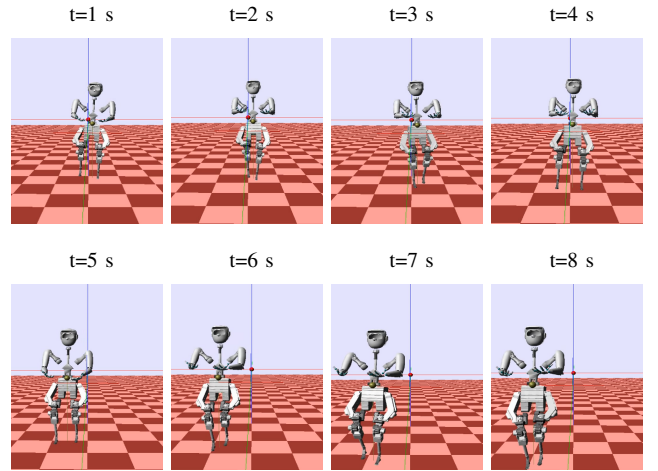


Fig. 6. Push recovery example: the robot walks forward at  $v_x = 0.2m/s$ , the pelvis is pushed at  $t = 3.7s$  by  $F = 200N$  during  $\Delta t = 0.1s$ .

torques for the whole body are computed using the hierarchical inverse dynamics described in Section IV.

In order to show the robustness of the proposed walking controller, we conduct different simulation experiments with various external disturbances. Since the robot has finite size feet (i.e. the CoP can move inside the foot), we set the current contact point  $u_0$  in our controller as the current CoP measurement at each control cycle. The constraints and physical properties are the same as for the LIPM experiments, except that the minimum step duration is now set to  $T_{min} = 0.3s$  to account for acceleration limits of the robot. We test two scenarios: push recovery and slippage recovery. In the first scenario, the pelvis is pushed during stepping in different directions and the performance of the controller is investigated. In the second scenario, the stance foot is pushed during stepping such that slippage occurs.

### A. Push recovery

We simulate the robot for the controller using fixed stepping duration and then with timing adaptation to better understand how step timing adaptation changes push recovery capabilities on the full humanoid. A typical side-step adaptation behavior is shown in Figure 6. In this figure, the robot walks forward at a desired speed,  $v_x = 0.2m/s$ . In this simulation, the robot

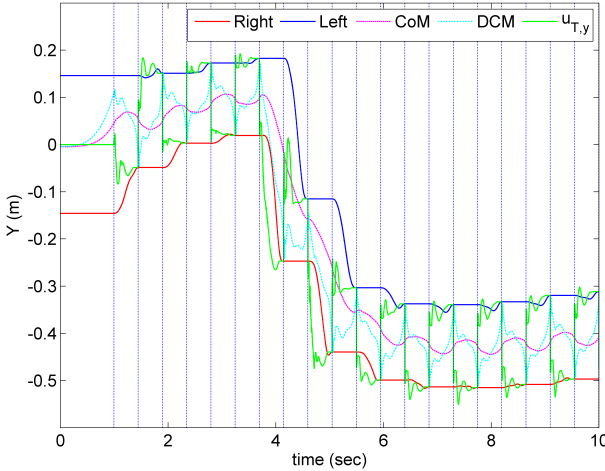


Fig. 7. First push recovery experiment: lateral trajectories during forward walking without step timing adjustment. The desired lateral velocity is zero in this simulation, however, when the push occurs ( $F = 200N$ , at  $t = 3.7s$  during  $\Delta t = 0.1s$  which causes an impulse of  $20 N \cdot s$ ), the controller sacrifices lateral velocity tracking to recover balance. This push ( $impulse = 20 N \cdot s$ ) is the maximum lateral (inward) disturbance that the robot could recover from without timing adjustment.

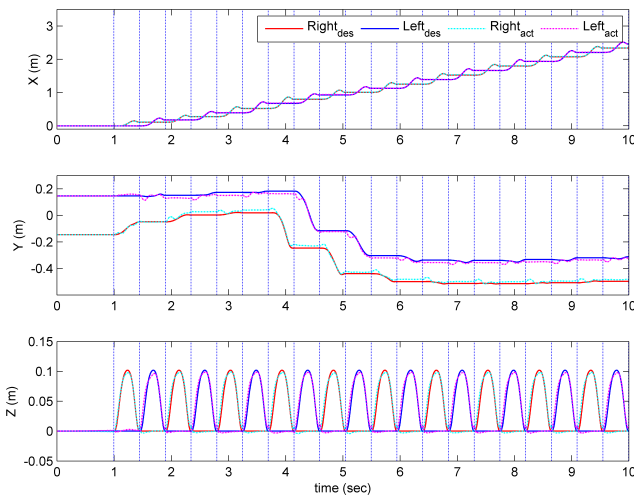


Fig. 8. First push recovery experiment: desired and actual feet trajectories during forward walking without step timing adjustment. The low-level controller tracks the smooth feet trajectories generated by our real-time walking controller.

pelvis is pushed to the right (inward direction) by a force  $F = 200 N$ , at  $t = 3.7 s$  during  $\Delta t = 0.1 s$  which creates a total impulse of  $20 N \cdot s$ . To recover from the push, the robot automatically starts stepping to the right direction. Once the push is rejected, the robot resumes its forward walking.

The push recovery capabilities of the controller without time adaptation are shown in Figure 7 and 8. The maximum lateral (inward) disturbance that the robot was able to withstand was a push of  $200 N$  for  $\Delta t = 0.1 s$ , i.e. an impulse of  $20 N \cdot s$ . As it can be seen in the figure, the feet trajectories are adapted to realize the desired landing locations. After the push, the controller sacrifices the lateral velocity tracking and adjusts the foot positions to recover balance. As it can be observed in Figure 8, the adapted trajectories of the feet are smooth, and the whole-body controller is able to track very well these

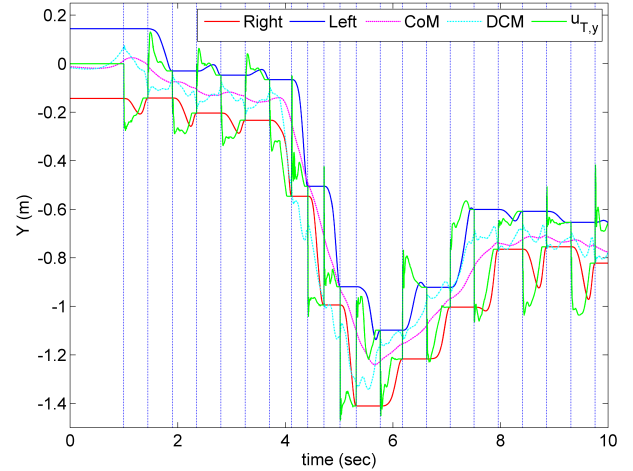


Fig. 9. Second push recovery experiment: The lateral trajectories during stepping in place with both step location and timing adjustment. The desired velocity is zero during this simulation. When the push ( $F = 390N$ , at  $t = 3.9s$  during  $\Delta t = 0.3s$ ) is exerted, the controller adapts both step location and timing to recover from this severe lateral (inward) push. This disturbance ( $impulse = 117 N \cdot s$ ) is the maximum lateral (inward) push that the robot could recover from with step timing adjustment in our simulations.

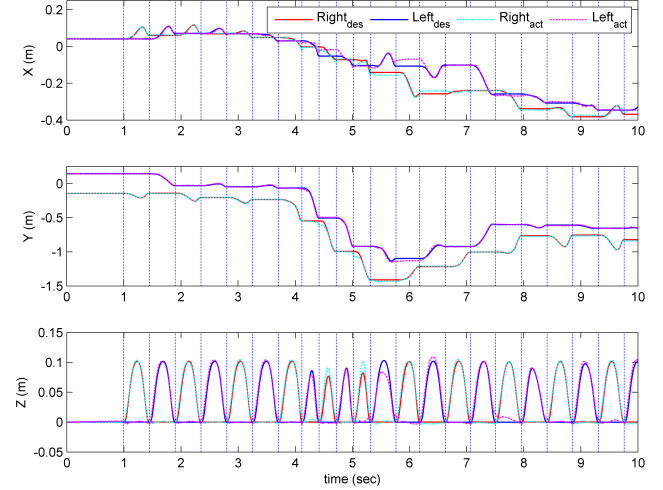


Fig. 10. Second push recovery experiment: The desired and actual feet trajectories during stepping in place with both step location and timing adjustment. The low-level controller tracks the smooth feet trajectories generated by our real-time walking controller. We can see that when the step timing is adapted, the step height is adapted to satisfy the constraints specified in (21).

trajectories.

The push recovery capabilities of the controller when step timing adaptation is enabled are shown in Figures 9 and 10. In this case, the maximum lateral (inward) disturbance that the robot was able to withstand was a push of  $390 N$  for  $\Delta t = 0.3 s$ , i.e. an impulse of  $117 N \cdot s$ , which is nearly six times the impulse that the robot could withstand when timing was not adapted. This is consistent with the results found for the LIP model (Figure 4 with  $\theta = -90$  deg). This result illustrates the importance of timing adaptation for stable walking. This important improvement can be intuitively explained by inspecting Equation (3) which shows that the DCM diverges as an exponential of time. As a result, taking fast steps (decreasing the step timing) causes exponential improvement to keep the DCM from diverging. This effect

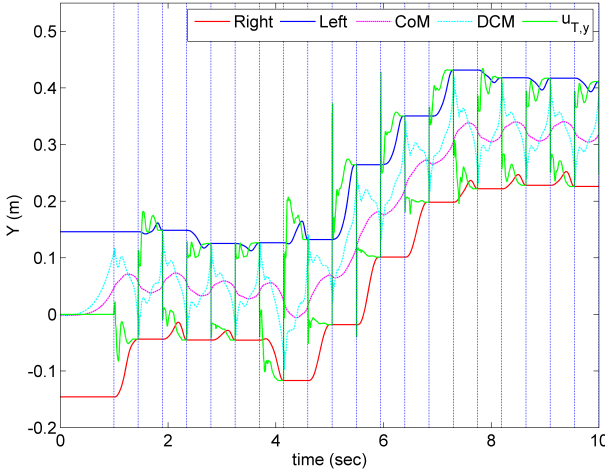


Fig. 11. First slippage recovery experiment: The lateral trajectories during a forward walking without step timing adjustment. The desired lateral velocity is zero during this simulation. The stance foot is pushed laterally by  $F = 400N$ , at  $t = 3.9s$  during  $\Delta t = 0.2s$  such that slippage occurs. After the push, the foot locations are adjusted to recover the robot from the push.

is magnified, when the robot takes several steps to recover from a disturbance.

We can see in Figure 9 that both step location and timing are adjusted. To recover from the push, the robot takes five steps with minimum step time to the left on the boundaries of the feasible area. The feet trajectories (Figure 10) are again adapted very smoothly in the case when step timing is adjusted. Furthermore, it can be observed that the step height is also adapted when the step duration is changed during push recovery. In fact, this shows that when step timing is adapted, the step height is adapted consistently with the constraints specified in Equation (21). The trajectory tracking in the vertical direction degrades compared to the case without timing adjustment (Figure 8). This is due to an increase in the desired swing foot acceleration. However, this performance for trajectory tracking in the vertical direction is good enough for realizing a feasible stepping.

### B. Slippage recovery

In the second scenario, we show the capability of our walking controller to recover from slippage. Here we note that walking controllers based on CoP modulation and tracking are usually very sensitive to foot slippage during walking. Indeed, when the stance foot slips, the CoP is not controllable anymore (like the case where the stance foot rotates around the edges). Here we aim to illustrate a benefit of our controller: since it does not rely on CoP control it can recover from large slippage by adjusting the swing foot landing location and time.

To cause foot slippage during walking, we apply strong pushes on the stance foot such that it slips. Note that the LIPM dynamics is not valid anymore during slipping. However, our controller constantly adapts the LIPM base,  $u_0$ , to the measured CoP which is sufficient for recovery.

Again, we compare the performance of the controller when step timing is adapted or not. For the case without timing adaptation, Figure 11 shows a forward walking simulation while the stance foot is pushed by  $F = 400N$ , at  $t = 3.9s$

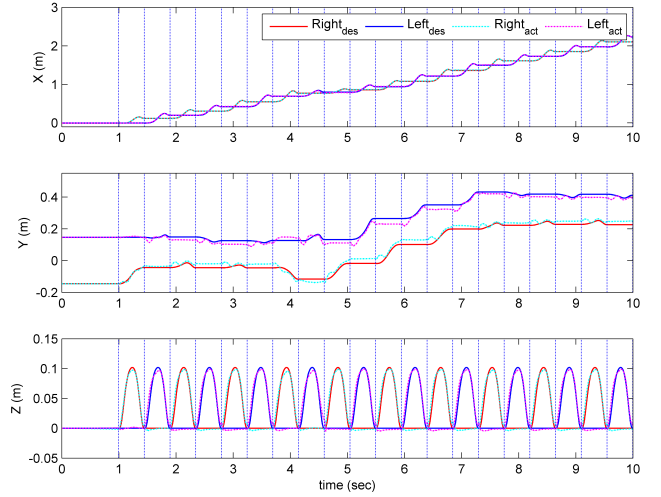


Fig. 12. First slippage recovery experiment: The desired and actual feet trajectories during a forward walking without step timing adjustment. When the push is exerted at  $t = 3.9s$ , the left foot slips to the left. The right foot trajectory is then adapted to recover the robot from this disturbance.

during  $\Delta t = 0.2s$  (impulse of  $80 N \cdot s$ ). Slippage of the left foot in this case can be observed in the actual foot trajectory in lateral direction in Figure 12. In this case, the left foot which is stance at  $t = 3.9s$  is pushed to the left. This causes a faster DCM divergence to the right direction. Hence, the right foot which is swing steps more in the right direction to recover from this disturbance.

Figure 13 shows the lateral trajectories for a simulation experiment with a push of  $F = 930N$ , at  $t = 3.9s$  during  $\Delta t = 0.3s$  (impulse of  $279 N \cdot s$ ) on the stance foot when step timing adjustment is enabled. Again, we can see a degradation in the foot trajectory tracking in lateral direction in Figure 14. In this case, the controller exploits a combination of step timing and location adjustment to recover from this strong disturbance. Furthermore, some high frequency oscillations can be seen in Figure 13 in the DCM trajectory (and the estimated next footprint), which is due to the huge disturbance on the stance foot. This huge disturbance causes high frequency oscillations of the passive elements in ankles. Here we note that the robot is able to withstand an impulse on the foot which is more than three times larger than the impulse withstood when step timing is not adjusted. This again illustrates the importance of timing adjustment during walking.

## VII. DISCUSSION

In this section, we discuss our results with respect to the state of the art and we outline the limitations of our approach.

### A. Results

The following points can be deduced from our experimental results:

- *Generality* Without modulating the CoP at each control cycle to control the CoM or DCM, we could generate robust gaits by adapting step timing and location. This suggests that our approach can be used for biped robots with active ankles, passive ankle, or point contact foot.

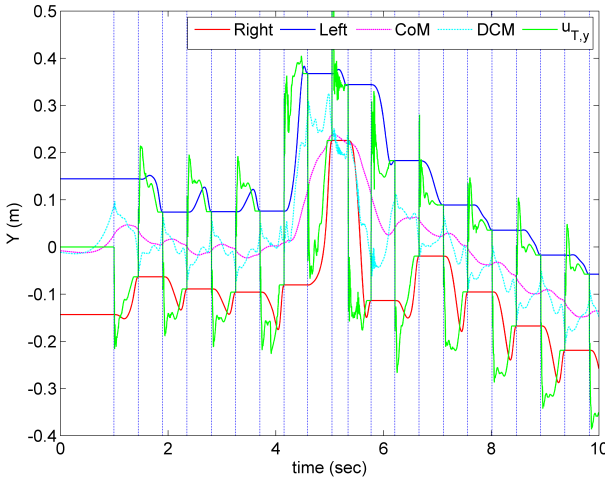


Fig. 13. Second slippage recovery experiment: The lateral trajectories during stepping in place with both step location and timing adjustment. The desired velocity is zero during this simulation. The stance foot is pushed laterally by  $F = 930N$ , at  $t = 3.9s$  during  $\Delta t = 0.3s$  such that slippage occurs. After the push, the foot locations are adjusted to recover the robot from the push. High frequency oscillations of the DCM trajectory is due to the huge disturbance on the stance foot. This huge disturbance causes high frequency oscillation of the passive elements in ankles.

We successfully used the controller to control an underactuated biped robot with passive ankle joints and prosthetic feet. Moreover, as we have discussed in Section II, optimizing for the DCM offset over one step is enough to always keep the robot in a viable state (if such a state exists).

- *Computational efficiency* The size of the optimization problem drastically decreases compared to an MPC approach with several preview steps. In fact, by considering the DCM offset as a decision variable in our optimization problem, we need not integrate the motion forward over several time steps to preserve a sufficient condition of viability [45]. This results in a very small sized QP compared to common optimization-based walking controllers [22], [43], [8], [15], typically at least an order of magnitude smaller in the number of decision variables.
- *Controller receding horizon length* A very interesting question that should be carefully answered by MPC-based walking controller designers is [47] : *how far ahead in time shall our controller optimize motion for?* We showed in this paper that by only looking at the end of the current step in the controller, the robot is able to recover walking from any viable state. Interestingly, analyses on human walking experiments agree with this argument for many cases such as normal walking with the change of step location and width and even in the presence of obstacles [37], [36]. Although, when walking becomes very challenging and constrained, such as walking on stepping stones, subjects look two steps ahead [36].
- *Importance of step timing adaptation* Our experiments show that timing adjustment significantly increases the walking robustness. Measuring the DCM enables us to adjust the step location in the direction of an external disturbance, while step timing adaptation helps us to regain the balance very fast. Since the DCM diverges

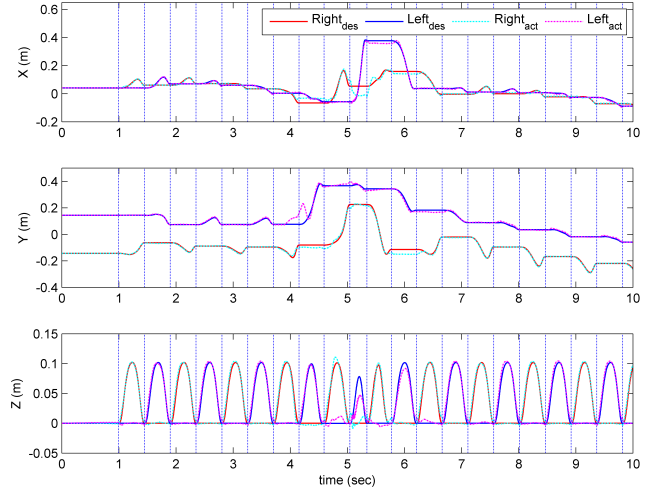


Fig. 14. Second slippage recovery experiment: The desired and actual feet trajectories during stepping in place with both step location and timing adjustment. When the push is exerted at  $t = 3.9s$ , the left foot slips to the left. The next steps locations are adapted to recover the robot from the disturbance.

exponentially with time, timing adjustment can improve robustness exponentially. This is the key point that shows the major role of timing adjustment in recovering from external disturbances. Fast recovery from large external disturbances with a full humanoid robot extends previous push recovery implementations that take one step [39], or several steps [12] without timing adaptation.

- *Robustness against various disturbances* The measured CoP and estimated DCM are employed to adapt the landing location and time of the swing foot but the controller does not try to control the CoP. This feature enabled us to conduct simulations with strong pushes on the pelvis and stance foot which cause rotation around the edges of the support polygon and foot slippage. In these cases the CoP is not controllable, however this does not degrade the performance of our controller. This feature might also enable the robot to walk over rough terrains, but this is left as a future work.

## B. Limitation

We discuss here the controller limitations and potential approaches to address them.

- *Timing constraint* Constraints on step locations are explicit and depend on the kinematic and environment limitations. However, constraints on step timing are a function of maximum acceleration of the swing foot as well as the distance between the current state of the swing foot and the landing location. As a result, considering a simple constraint on step timing for the worst case decreases the performance of the controller. To circumvent this, we can employ more complex models (but linear) which take into account the swing foot dynamics [40]. Using such models, we could directly constrain the swing foot acceleration instead of step timing.
- *Angular momentum* We used the LIPM to derive a walking controller, which assumes zero angular momentum

and fixed CoM height. This model has been successfully used for online walking pattern generators over a wide range of terrains in numerous previous contributions. However, considering angular momentum dynamics could improve the range of external disturbances that can be handled by the controller. In order to keep the constraints linear, we could employ the LIP with flywheel model [38] and use the angular momentum as a decision variable in the optimization problem.

- *Walking on stepping stones or in scattered environments* We showed that we do not need to consider a horizon in our walking controller to guarantee viability of the motion. However, when the feasible foot locations are very limited by the environment, such as walking over stepping stones or in the presence of obstacles, we need to add a horizon in the controller to steer the DCM motion in the direction of safe contact points. This problem can be tackled without adding considerable computational burden to our walking controller. Our suggestion is to adapt step timing only in the first step within a desired horizon and to optimize for the subsequent step locations with a fixed nominal step timing. The derivation of such controller is straightforward from the formalism proposed in the paper.
- *Real robot experiments* Previous works [11], [39] have shown that our modeling assumptions can be successfully used on a real robot. While this suggests that our approach would work as well, real robot experiments, especially for robots with passive ankles or point feet would be most valuable. At the time when the research was conducted, we did not have access to such robots.

## VIII. CONCLUSION

In this paper, we proposed a walking controller that adapts both step location and timing in real time to generate robust gaits. In the case of the LIPM, the controller is guaranteed to recover from any disturbances as long as the current state is viable by solely considering the next step location and timing. Comparison with state of the art preview controllers emphasized the importance of step timing adaptation and demonstrated that our approach can be significantly more robust than methods that do not adjust timing, even when those controllers optimize over several preview steps. Full humanoid simulations through push recovery and slippage recovery scenarios on a biped robot with passive ankles showed the robustness of our proposed controller even without control authority in the ankles.

## ACKNOWLEDGMENT

This research was supported by the Max-Planck Society, MPI-ETH center for learning systems and the European Research Council under the European Union's Horizon 2020 research and innovation program (grant agreement No 637935).

## REFERENCES

- [1] Z. Aftab, T. Robert, and P.-B. Wieber, “Ankle, hip and stepping strategies for humanoid balance recovery with a single model predictive control scheme,” in *2012 12th IEEE-RAS International Conference on Humanoid Robots (Humanoids 2012)*. IEEE, 2012, pp. 159–164.
- [2] J.-P. Aubin, “Viability theory. systems & control: Foundations & applications,” *Birkhäuser, Boston*. doi, vol. 10, no. 1007, pp. 978–0, 1991.
- [3] T. Buschmann, S. Lohmeier, M. Bachmayer, H. Ulbrich, and F. Pfeiffer, “A collocation method for real-time walking pattern generation,” in *2007 7th IEEE-RAS International Conference on Humanoid Robots*. IEEE, 2007, pp. 1–6.
- [4] S. Caron and A. Kheddar, “Dynamic walking over rough terrains by nonlinear predictive control of the floating-base inverted pendulum,” *arXiv preprint arXiv:1703.00688*, 2017.
- [5] S. Caron and Q.-C. Pham, “When to make a step? tackling the timing problem in multi-contact locomotion by topp-mpc,” *arXiv preprint arXiv:1609.04600*, 2016.
- [6] J. Carpentier, S. Tonneau, M. Naveau, O. Stasse, and N. Mansard, “A Versatile and Efficient Pattern Generator for Generalized Legged Locomotion,” in *IEEE International Conference on Robotics and Automation (ICRA)*, Stockholm, Sweden, May 2016.
- [7] J. A. Castano, Z. Li, C. Zhou, N. Tsagarakis, and D. Caldwell, “Dynamic and reactive walking for humanoid robots based on foot placement control,” *International Journal of Humanoid Robotics*, vol. 13, no. 02, p. 1550041, 2016.
- [8] H. Diedam, D. Dimitrov, P.-B. Wieber, K. Mombaur, and M. Diehl, “Online walking gait generation with adaptive foot positioning through linear model predictive control,” in *2008 IEEE/RSJ International Conference on Intelligent Robots and Systems*. IEEE, 2008, pp. 1121–1126.
- [9] J. Englsberger, C. Ott, and A. Albu-Schäffer, “Three-dimensional bipedal walking control using divergent component of motion,” in *Intelligent Robots and Systems (IROS), 2013 IEEE/RSJ International Conference on*. IEEE, 2013, pp. 2600–2607.
- [10] J. Englsberger, C. Ott, and A. Albu-Schäffer, “Three-dimensional bipedal walking control based on divergent component of motion,” *IEEE Transactions on Robotics*, vol. 31, no. 2, pp. 355–368, 2015.
- [11] S. Feng, “Online hierarchical optimization for humanoid control,” Ph.D. dissertation, Carnegie Mellon University, 2016.
- [12] S. Feng, X. Xinjilefu, C. G. Atkeson, and J. Kim, “Robust dynamic walking using online foot step optimization,” in *Intelligent Robots and Systems (IROS), 2016 IEEE/RSJ International Conference on*. IEEE, 2016, pp. 5373–5378.
- [13] R. J. Griffin, G. Wiedebach, S. Bertrand, A. Leonessa, and J. Pratt, “Walking stabilization using step timing and location adjustment on the humanoid robot, atlas,” *arXiv preprint arXiv:1703.00477*, 2017.
- [14] K. Harada, S. Kajita, K. Kaneko, and H. Hirukawa, “An analytical method for real-time gait planning for humanoid robots,” *International Journal of Humanoid Robotics*, vol. 3, no. 01, pp. 1–19, 2006.
- [15] A. Herdt, H. Diedam, P.-B. Wieber, D. Dimitrov, K. Mombaur, and M. Diehl, “Online walking motion generation with automatic footstep placement,” *Advanced Robotics*, vol. 24, no. 5-6, pp. 719–737, 2010.
- [16] A. Herdt, N. Perrin, and P.-B. Wieber, “Walking without thinking about it,” in *Intelligent Robots and Systems (IROS), 2010 IEEE/RSJ International Conference on*. IEEE, 2010, pp. 190–195.
- [17] A. Herzog, N. Rotella, S. Mason, F. Grimminger, S. Schaal, and L. Righetti, “Momentum control with hierarchical inverse dynamics on a torque-controlled humanoid,” *Autonomous Robots*, vol. 40, no. 3, pp. 473–491, 2016.
- [18] A. Herzog, N. Rotella, S. Schaal, and L. Righetti, “Trajectory generation for multi-contact momentum control,” in *Humanoid Robots (Humanoids), 2015 IEEE-RAS 15th International Conference on*. IEEE, 2015, pp. 874–880.
- [19] A. Herzog, S. Schaal, and L. Righetti, “Structured contact force optimization for kino-dynamic motion generation,” in *Intelligent Robots and Systems (IROS), 2016 IEEE/RSJ International Conference on*. IEEE, 2016, pp. 2703–2710.
- [20] A. L. Hof, “The extrapolated center of mass concept suggests a simple control of balance in walking,” *Human movement science*, vol. 27, no. 1, pp. 112–125, 2008.
- [21] C. Hubicki, J. Grimes, M. Jones, D. Renjewski, A. Spröwitz, A. Abate, and J. Hurst, “Atrias: Design and validation of a tether-free 3d-capable spring-mass bipedal robot,” *The International Journal of Robotics Research*, p. 0278364916648388, 2016.
- [22] S. Kajita, F. Kanehiro, K. Kaneko, K. Fujiwara, K. Harada, K. Yokoi, and H. Hirukawa, “Biped walking pattern generation by using preview control of zero-moment point,” in *Robotics and Automation (ICRA), IEEE International Conference on*. IEEE, 2003, pp. 1620–1626.
- [23] S. Kajita, F. Kanehiro, K. Kaneko, K. Yokoi, and H. Hirukawa, “The 3d linear inverted pendulum mode: A simple modeling for a biped walking pattern generation,” in *Intelligent Robots and Systems, IEEE/RSJ International Conference on*. IEEE, 2001, pp. 239–246.

[24] M. Khadiv, A. Herzog, S. A. A. Moosavian, and L. Righetti, "Step timing adjustment: A step toward generating robust gaits," in *Humanoid Robots (Humanoids), 2016 IEEE-RAS 16th International Conference on*. IEEE, 2016, pp. 35–42.

[25] M. Khadiv, S. Kleff, A. Herzog, S. A. A. Moosavian, S. Schaal, and L. Righetti, "Stepping stabilization using a combination of dcm tracking and step adjustment," in *Robotics and Mechatronics (ICRoM), 2016 4th RSI International Conference on*, Available: <https://arxiv.org/abs/1609.09822v1>, 2016.

[26] M. Khadiv, S. A. A. Moosavian, A. Yousefi-Koma, H. Maleki, and M. Sadedel, "Online adaptation for humanoids walking on uncertain surfaces," *Proc IMechE Part I: Journal of Systems and Control Engineering (accepted)*, Available: <https://arxiv.org/abs/1703.10337>, 2017.

[27] M. Khadiv, S. A. A. Moosavian, A. Yousefi-Koma, M. Sadedel, and S. Mansouri, "Optimal gait planning for humanoids with 3d structure walking on slippery surfaces," *Robotica*, vol. 35, no. 3, pp. 569–587, 2017.

[28] T. Koolen, T. De Boer, J. Rebula, A. Goswami, and J. Pratt, "Capturability-based analysis and control of legged locomotion, part 1: Theory and application to three simple gait models," *The International Journal of Robotics Research*, vol. 31, no. 9, pp. 1094–1113, 2012.

[29] P. Kryczka, P. Kormushev, N. G. Tsagarakis, and D. G. Caldwell, "Online regeneration of bipedal walking gait pattern optimizing footstep placement and timing," in *Intelligent Robots and Systems (IROS), 2015 IEEE/RSJ International Conference on*. IEEE, 2015, pp. 3352–3357.

[30] S. Lengagne, J. Vaillant, E. Yoshida, and A. Kheddar, "Generation of whole-body optimal dynamic multi-contact motions," *The International Journal of Robotics Research*, vol. 32, no. 9-10, pp. 1104–1119, 2013.

[31] M. R. Maximo, C. H. Ribeiro, and R. J. Afonso, "Mixed-integer programming for automatic walking step duration," in *Intelligent Robots and Systems (IROS), 2016 IEEE/RSJ International Conference on*. IEEE, 2016, pp. 5399–5404.

[32] M. Missura and S. Behnke, "Omnidirectional capture steps for biped walking," in *Humanoid Robots (Humanoids), 2013 13th IEEE-RAS International Conference on*. IEEE, 2013, pp. 14–20.

[33] I. Mordatch, E. Todorov, and Z. Popović, "Discovery of complex behaviors through contact-invariant optimization," *ACM Transactions on Graphics (TOG)*, vol. 31, no. 4, p. 43, 2012.

[34] M. Morisawa, K. Harada, S. Kajita, K. Kaneko, F. Kanehiro, K. Fujiwara, S. Nakaoka, and H. Hirukawa, "A biped pattern generation allowing immediate modification of foot placement in real-time," in *2006 6th IEEE-RAS International Conference on Humanoid Robots*. IEEE, 2006, pp. 581–586.

[35] I.-W. Park, J.-Y. Kim, J. Lee, and J.-H. Oh, "Online free walking trajectory generation for biped humanoid robot khr-3 (hubo)," in *Robotics and Automation, 2006. ICRA 2006. Proceedings 2006 IEEE International Conference on*. IEEE, 2006, pp. 1231–1236.

[36] A. E. Patla and J. Vickers, "How far ahead do we look when required to step on specific locations in the travel path during locomotion?" *Experimental brain research*, vol. 148, no. 1, pp. 133–138, 2003.

[37] A. E. Patla and J. N. Vickers, "Where and when do we look as we approach and step over an obstacle in the travel path?" *Neuroreport*, vol. 8, no. 17, pp. 3661–3665, 1997.

[38] J. Pratt, J. Carff, S. Drakunov, and A. Goswami, "Capture point: A step toward humanoid push recovery," in *2006 6th IEEE-RAS international conference on humanoid robots*. IEEE, 2006, pp. 200–207.

[39] J. Pratt, T. Koolen, T. De Boer, J. Rebula, S. Cotton, J. Carff, M. Johnson, and P. Neuhaus, "Capturability-based analysis and control of legged locomotion, part 2: Application to m2v2, a lower body humanoid," *The International Journal of Robotics Research*, p. 0278364912452762, 2012.

[40] T. Takenaka, T. Matsumoto, and T. Yoshiike, "Real time motion generation and control for biped robot-1 st report: Walking gait pattern generation," in *2009 IEEE/RSJ International Conference on Intelligent Robots and Systems*. IEEE, 2009, pp. 1084–1091.

[41] Y. Tassa, T. Erez, and E. Todorov, "Synthesis and stabilization of complex behaviors through online trajectory optimization," in *Intelligent Robots and Systems (IROS), 2012 IEEE/RSJ International Conference on*. IEEE, 2012, pp. 4906–4913.

[42] P.-B. Wieber, "On the stability of walking systems," in *Proceedings of the international workshop on humanoid and human friendly robotics*, 2002.

[43] P. B. Wieber, "Trajectory free linear model predictive control for stable walking in the presence of strong perturbations," in *2006 6th IEEE-RAS International Conference on Humanoid Robots*. IEEE, 2006, pp. 137–142.

[44] P.-B. Wieber, "Viability and predictive control for safe locomotion," in *2008 IEEE/RSJ International Conference on Intelligent Robots and Systems*. IEEE, 2008, pp. 1103–1108.

[45] P.-B. Wieber, R. Tedrake, and S. Kuindersma, "Modeling and control of legged robots," in *Springer Handbook of Robotics*. Springer, 2016, pp. 1203–1234.

[46] A. W. Winkler, C. D. Bellicoso, M. Hutter, and J. Buchli, "Gait and trajectory optimization for legged systems through phase-based end-effector parameterization," *IEEE Robotics and Automation Letters*, vol. 3, no. 3, pp. 1560–1567, 2018.

[47] P. Zaytsev, S. J. Hasaneini, and A. Ruina, "Two steps is enough: no need to plan far ahead for walking balance," in *Robotics and Automation (ICRA), 2015 IEEE International Conference on*. IEEE, 2015, pp. 6295–6300.

## APPENDIX A: DERIVATION OF EQUATION (7)

Using Equations (4) and (5), we can write the LIPM equations in terms of the DCM offset and the next step location

$$u_T = (\xi_0 - u_0)e^{\omega_0 T} + u_0 - b \quad (27)$$

For a constant walking velocity, the desired DCM offset in the sagittal direction,  $b_x$ , is considered to be constant over several steps, therefore we have

$$u_{T,x} = b_x e^{\omega_0 T} + u_{0,x} - b_x \quad (28)$$

since  $L = u_{T,x} - u_{0,x}$  over two consecutive steps, we have

$$b_x = \frac{L}{e^{\omega_0 T} - 1} \quad (29)$$

Note that this DCM offset can be seen as a fixed point of the dynamics, in the sense that keeping  $L$  and  $T$  constant over several steps will lead to steady state forward walking velocity.

For a desired sideward walking, the distance between the feet is equal to  $l_p + W$  or  $l_p - W$  as shown in Figure 1. Using (27), we can write down the equations for the right and left foot DCM offset

$$\begin{aligned} -(l_p - W) &= b_{y,r} e^{\omega_0 T} - b_{y,r} \\ l_p + W &= b_{y,r} e^{\omega_0 T} - b_{y,l} \end{aligned} \quad (30)$$

Solving (31) for  $b_{y,r}$  and  $b_{y,l}$  yields:

$$\begin{aligned} b_{y,r} &= \frac{l_p}{1 + e^{\omega_0 T}} - \frac{W}{1 - e^{\omega_0 T}} \\ b_{y,l} &= -\frac{l_p}{1 + e^{\omega_0 T}} - \frac{W}{1 - e^{\omega_0 T}} \end{aligned} \quad (31)$$

Introducing  $n$  as the index for distinguishing the left and right foot ( $n = 1$  when the right foot is stance, and  $n = 2$  when the left foot is stance), the DCM offset in the latter direction can be written down as:

$$b_y = (-1)^n \frac{l_p}{1 + e^{\omega_0 T}} - \frac{W}{1 - e^{\omega_0 T}} \quad (32)$$

## APPENDIX B: VIABILITY IN THE LATERAL DIRECTION

Since in the lateral direction the feasible area for stepping is not symmetric with respect to the stance foot (due to self collision), the maximum allowable DCM offsets for outward and inward directions are different. It should be noted that we use outward for the direction that the legs are prone to experience a self collision, and inward for the opposite

direction. We hypothesis that the maximum allowable DCM offsets in these directions are:

$$b_{y,max,out} = \frac{l_p}{1 + e^{\omega_0 T_{min}}} + \frac{W_{max} - W_{min} e^{\omega_0 T_{min}}}{1 - e^{2\omega_0 T_{min}}} \quad (33a)$$

$$b_{y,max,in} = \frac{l_p}{1 + e^{\omega_0 T_{min}}} + \frac{W_{min} - W_{max} e^{\omega_0 T_{min}}}{1 - e^{2\omega_0 T_{min}}} \quad (33b)$$

To show that these values exactly split state space into the viable and non-viable parts, we again investigate the situations where the DCM offsets are less or more than these values for both outward and inward directions. We conduct this analysis for the case where the right foot is stance, while for the other case the same results are obtained.

Considering a DCM offset more (less) than the value in (33a) for outward direction at the start of a step (where the right foot is stance) as:

$$\xi_{y,0} - u_{y,0} = \frac{l_p}{1 + e^{\omega_0 T_{min}}} + \frac{W_{max} - W_{min} e^{\omega_0 T_{min}}}{1 - e^{2\omega_0 T_{min}}} \pm \epsilon \quad (34)$$

the minimum feasible DCM offset at the end of this step ( $b_{y,T}$ ) is obtained taking a step with the minimum step width (for avoiding self collision) at the minimum step time using (27):

$$b_{y,T} = \left( \frac{l_p}{1 + e^{\omega_0 T_{min}}} + \frac{W_{max} - W_{min} e^{\omega_0 T_{min}}}{1 - e^{2\omega_0 T_{min}}} \pm \epsilon \right) e^{\omega_0 T_{min}} - (l_p + W_{min}) \quad (35)$$

Using this value as the DCM offset at the start of next step, and taking a step with the maximum step width at the minimum step time yield the minimum feasible DCM offset of the next step:

$$b_{y,2T} = \left( \frac{l_p}{1 + e^{\omega_0 T_{min}}} + \frac{W_{max} - W_{min} e^{\omega_0 T_{min}}}{1 - e^{2\omega_0 T_{min}}} \pm \epsilon \right) e^{2\omega_0 T_{min}} - (l_p + W_{min}) e^{\omega_0 T_{min}} + (l_p + W_{max}) \quad (36)$$

Simplifying (36) yields:

$$b_{y,2T} = \frac{l_p}{1 + e^{\omega_0 T_{min}}} + \frac{W_{max} - W_{min} e^{\omega_0 T_{min}}}{1 - e^{2\omega_0 T_{min}}} \pm \epsilon e^{2\omega_0 T_{min}} \quad (37)$$

Comparing (34) with (37) reveals that starting from a DCM offset more than the value in (33a) (positive  $\epsilon$  in (34)) and after taking two steps on the boundaries of the feasible area at the minimum time, the DCM offset increases by a factor  $e^{2\omega_0 T_{min}}$  times  $\epsilon$ . As a result, any DCM offset more than the value in (33a) for outward direction causes divergence. However, starting from a DCM offset less than the value in (33a) (negative  $\epsilon$  in (34)), there exists one evolution (stepping on the boundaries of the feasible area at the minimum time) that keeps the DCM from diverging. Hence, we can conclude that the value in (33a) for outward direction exactly splits state space into the viable and non-viable parts. Similar procedure can be done for inward direction starting with (33b).



**Majid Khadiv** is a postdoc scholar at the Movement Generation and Control Group at the Max-Planck Institute for Intelligent Systems. He received his BSc degree in Mechanical Engineering from Isfahan University of Technology (IUT), in 2010, and his Msc and PhD degree in Mechanical Engineering from K. N. Toosi University of Technology, Tehran, Iran in 2012 and 2017. Majid joined the Iranian national humanoid project, Surena III, and worked as the head of dynamics and control group from 2012 to 2015. He also spent a one-year visiting

scholarship under supervision of Dr. Ludovic Righetti at the Autonomous Motion Laboratory (AMD), Max-Planck Institute for Intelligent Systems. His research interests include planning and control of legged robots especially humanoids.



**Alexander Herzog** is a roboticist at X, Inc. (Google). He did his PhD at the Max Planck Institute for Intelligent Systems, Tübingen and received his doctorate degree from ETH Zürich. Dr Herzog studied Computer-Science at the Karlsruhe Institute of Technology, in Germany. He visited the Computational Learning and Motor Control Lab (University of Southern California) regularly from 2011 to 2016 where he collaborated in projects on grasp learning and locomotion for humanoid robots. After receiving his Diploma in 2011, he joined the Autonomous Motion Laboratory at the Max-Planck Institute for Intelligent Systems in 2012. During his PhD he worked on contact interaction in whole-body control and grasping for humanoids.



**S. Ali. A. Moosavian** received his B.Sc. degree in 1986 from Sharif University of Technology and the M.Sc. degree in 1990 from Tarbiat Modares University (both in Tehran), and his Ph.D. degree in 1996 from McGill University (Montreal, Canada), all in Mechanical Engineering. He is a Professor with the Mechanical Engineering Department at K. N. Toosi University of Technology (KNTU) in Tehran since 1997. His research interests are in the areas of dynamics modeling and motion/impedance control of terrestrial, legged and space robotic systems. He has published more than 200 articles in peer-reviewed journals and conference proceedings. He is a Member of IEEE, and one of the Founders of the ARAS Research Group, and the Manager of Center of Excellence in Robotics and Control at KNTU.



**Ludovic Righetti** is an Associate Professor in the Electrical and Computer Engineering Department and in the Mechanical and Aerospace Engineering Department at the Tandon School of Engineering at New York University and a Senior Researcher at the Max-Planck Institute for Intelligent Systems in Tübingen, Germany. He holds an engineering diploma in Computer Science (2004) and a Doctorate in Science (2008) from the Ecole Polytechnique Fédérale de Lausanne (Switzerland). He was a postdoctoral fellow at the University of Southern California from 2009 to 2012 and started the Movement Generation and Control Group at the Max-Planck Institute for Intelligent Systems in 2012. His research focuses on the planning and control of movements for autonomous robots, with a special emphasis on legged locomotion and manipulation.